

## INTERACTION OF SO<sub>2</sub> AND NO<sub>x</sub> WITH SOOT

A. R. Chughtai, M. M. O. Atteya, B. K. Konowalchuk,  
M. L. Rosenberger, and D. M. Smith  
Department of Chemistry, University of Denver  
Denver, CO 80208

Keywords: SO<sub>2</sub>, NO<sub>x</sub>, Soot

### INTRODUCTION

As part of a continuing study of the heterogeneous reactions of black carbon with gas phase oxidant species, the adsorption of low concentrations (30 - 2000 ppm) of SO<sub>2</sub> and NO<sub>x</sub> individually, together, and in the presence of other adsorbates have been studied by spectroscopic and microgravimetric techniques. Previous work in this study has revealed a dual path mechanism for the reaction of NO<sub>x</sub>/N<sub>2</sub>O<sub>4</sub> with n-hexane soot over concentration range 9 ppm - 200 torr (1,2). (This soot has been used throughout these investigations as a model for fossil fuel-produced black carbon). The effect of simulated solar radiation on the reaction at lower pressures (9-35ppm) is in the diminution of the NO<sub>x</sub> reactant through its photolytic dissociation (2). An FT-IR study of the reaction of various nitrogen oxides with black carbon showed the only reactive species at 298K to be NO<sub>x</sub> with NO and N<sub>2</sub>O unreactive (3). A spectroscopic examination of the gaseous products of the soot-oxides of nitrogen-water vapor reaction has revealed the formation of CO, CO<sub>2</sub>, and N<sub>2</sub>O, along with NO, from a redox reaction between NO<sub>x</sub>/N<sub>2</sub>O<sub>4</sub> and the most reactive components of soot during the reaction's early stages (4). At higher temperatures and NO<sub>x</sub>/N<sub>2</sub>O<sub>4</sub> pressures, n-hexane soot undergoes chemisorption and two types of redox reaction depending upon the conditions (5). The major redox reaction, for which an intermediate C-(NO<sub>x</sub>)<sub>x</sub> complex has been identified, is precluded by prior chemisorption but, if initiated, results in brisk oxidation of the carbon to CO and CO<sub>2</sub> (5). Previous studies of black carbon-SO<sub>2</sub>-H<sub>2</sub>O-O<sub>2</sub> reaction systems in these laboratories include the effect of simulated solar radiation in the formation of surface sulfate (6) and the effect of metal oxides with carbon on sulfate formation (7). Interaction of SO<sub>2</sub> and carbon represent the most intensively studied of the heterogeneous systems containing carbon. An attempt to understand the molecular dynamics involved in the reactions of carbon in the presence of multiple reactants, such as SO<sub>2</sub> and NO<sub>x</sub>, underlies the present work.

### RESULTS AND DISCUSSION

#### SO<sub>2</sub> Adsorption

Because those reactions of SO<sub>2</sub> and NO<sub>x</sub> in the presence of and with black carbon which are of interest to us occur in air, all adsorption studies were carried out in the presence of zero air (compressed air with CO<sub>2</sub> and H<sub>2</sub>O removed). This immediately raises the question of any role of O<sub>2</sub> in SO<sub>2</sub> adsorption, one addressed in our other paper in this symposium (8), involving competition for adsorption sites. That work demonstrates no such direct competition, or at least weaker adsorption of SO<sub>2</sub>, the presence of SO<sub>2</sub> showing no effect on the corrected normalized integral of soot's EPR signal (8).

Microgravimetric experiments in which 10 mg n-hexane soot was exposed to 600-2000 ppm SO<sub>2</sub> show a depletive adsorption as illustrated in Figure 1. At 60 min., just prior to the purge with zero air, the surface coverages (θ) by SO<sub>2</sub> were calculated from soot mass increase, its specific surface area of 89±2 m<sup>2</sup>/g, and a molecular area for SO<sub>2</sub> of 19.2 Å<sup>2</sup>(9), for each replicate run. A plot of θ versus P<sub>SO<sub>2</sub></sub> shows a linear dependence, Figure 2, for which the relationship

$$\theta = (5.06 \pm 0.07) \times 10^{-5} P_{SO_2} + (18.16 \pm 0.08) \times 10^{-2} \quad (1)$$

obtains. A linear relationship between θ and P is expected at low pressures for adsorption systems obeying the Langmuir isotherm (10)

$\theta = kP/(1+kP)$  (2)

The intercept in this case suggests a second mode of  $SO_2$  adsorption which may be determined by some surface

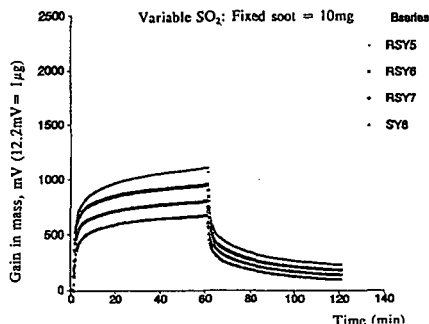


Figure 1. Adsorption of  $SO_2$  on soot

characteristic. Independent evidence of another mode comes from Figure 1 in which the desorption of  $SO_2$  by zero air asymptotically approaches a limiting mass reflecting retention of as much as 20% of the total adsorbed. A likely candidate for

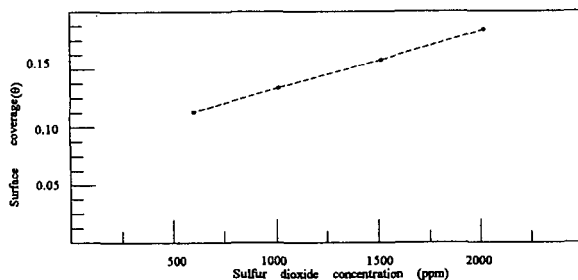
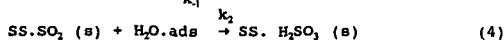
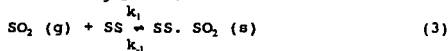
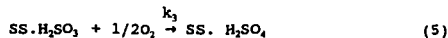


Figure 2. Plot of surface coverage ( $\theta$ ) as a function of  $P_{SO_2}$

this adsorption pathway is the surface hydrolysis of  $SO_2$  to  $SO_2 \cdot H_2O$  ( $H_2SO_3$ ). The resulting reaction scheme



where SS = surface site, could be followed by oxidation to sulfate



Small amounts of adsorbed water cannot be excluded from the soot surface under these conditions.

The effect of temperature on  $SO_2$  adsorption was examined with a soot mass of 15 mg at 1010 ppm  $SO_2$  by the same microgravimetric technique. Figure 3 shows a family of mass gain versus time curves over the temperature range 22°C to 66°C for the first 5

minutes of the adsorption experiment. These data represent surface coverages ranging from 8.6 to 2.2 percent, respectively, which exhibit a linear relationship to temperature. Utilizing microgravimetric data such as those of Figure 1, it is possible to estimate the fraction of adsorbed  $\text{SO}_2$  which is irreversibly bound to the surface, as represented by equation 4,

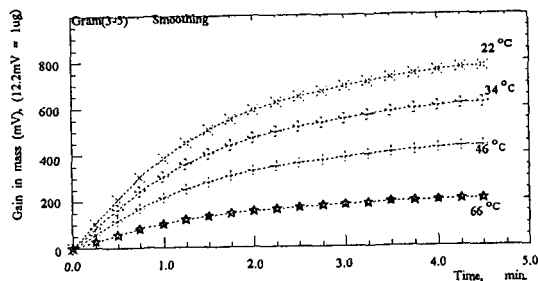


Figure 3. Mass gain versus time curves as a function of temperature.

at each temperature. From the total number of adsorbed molecules per gram, then, the reversibly adsorbed (physisorbed)  $\text{SO}_2$  and a set of equilibrium constants for equation 3 have been calculated. These data are summarized in Table I.

Table I. Effect of Temperature on  $\text{SO}_2$  Adsorption

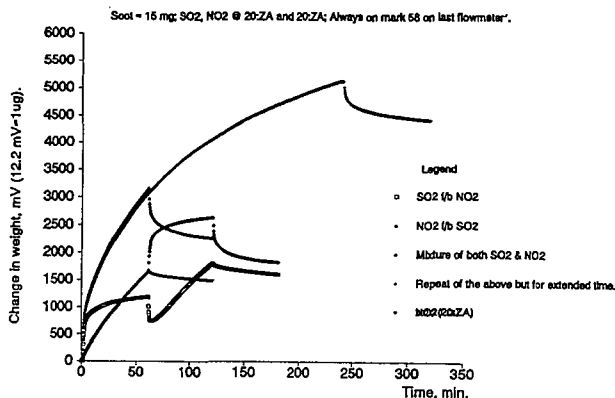
Temperature, °C	$\text{SO}_2$ Surface Coverage, $\theta$	Fraction of $\text{SO}_2$ physisorbed, $f$	$K_a \times 10^{16}$ , molecules per g-ppm
22	0.0858	0.823	3.24
34	0.0684	0.810	2.54
46	0.0479	0.772	1.74
66	0.0225	0.763	0.79

Plots of  $\log K_a$  versus  $1/T$  show some curvature reflecting the apparent fact that the enthalpy of physisorption for  $\text{SO}_2$  on n-hexane soot is a function of surface coverage. Over the temperature range 22–66°C, this value averages 26.8 kJ/mol-K, a figure within the range of 20–27 kJ/mol found by Davini (11) for  $\text{SO}_2$  adsorption on three oxidized carbons at 20°C and 1 atmosphere. By comparison, the molar heat of vaporization of  $\text{SO}_2$  also is 26.8 kJ/mol at 22°C.

#### Coadsorption of $\text{SO}_2$ and $\text{NO}_2$

Spectroscopic and microgravimetric data from the  $\text{NO}_2/\text{N}_2\text{O}_5$ -soot system (1,2) over a wide concentration range conform to the Elovich equation, an isotherm for activated adsorption or chemisorption. The principal products at low concentration of  $\text{NO}_2$  at laboratory temperatures are such functional groups as  $-\text{NO}_2$ ,  $-\text{ONO}$ ,  $-\text{NNO}_2$ . As noted above, on the other hand,  $\text{SO}_2$  adsorption is primarily reversible, involves a low heat of adsorption and is more properly termed physisorption; however, up to 20% appears to be surface reactive or undergoes some type of chemisorption. Of interest in this work have been the molecular mechanisms of coadsorption of  $\text{SO}_2$  and  $\text{NO}_2$ , given the different natures of their adsorption.

Figure 4 is a composite of microgravimetric curves of soot which summarizes its behavior during a series of  $\text{SO}_2$  and  $\text{NO}_2$  exposures.



Each experiment was carried out with 15 mg soot and 1010 ppm of SO<sub>2</sub> and \ or NO<sub>2</sub> in zero air at 22°C. This sequence of curves reveals the following:

1. the typical SO<sub>2</sub> adsorption curve is interrupted by a flow of NO<sub>2</sub> at 60 min, the SO<sub>2</sub> desorption (as P<sub>SO<sub>2</sub></sub> → 0) followed within 4 minutes by the increase in mass accompanying NO<sub>2</sub> chemisorption;
2. the inverse order of flow shows an adsorption of SO<sub>2</sub> following NO<sub>2</sub> of about 16% less than untreated soot; because NO<sub>2</sub> is mostly chemisorbed, the SO<sub>2</sub> flow does not result in visible mass loss;
3. a flow of SO<sub>2</sub> and NO<sub>2</sub> together yields an increase in mass 11% higher than separately; this curve is reproduced over the longer term, with the loss of mass (mostly SO<sub>2</sub>) about the same in each case when the same zero air purge is used;
4. small amounts of NO<sub>2</sub> are lost through zero air purge, indicating a small amount (9.7%) of NO<sub>2</sub> is loosely bound (physisorbed) under these conditions.

EPR measurements of spin density, the principles of which are discussed in our first symposium paper (8), have been carried out on this system as well, and the results are summarized in Figure 5. The decrease in corrected normalized integral (CNI) of soot's EPR signal with the pressure of paramagnetic NO<sub>2</sub> is evident as is the lack of effect of diamagnetic SO<sub>2</sub>. When experiments in which SO<sub>2</sub> adsorption is followed by NO<sub>2</sub> adsorption and vice-versa are carried out, there clearly is no effect of the presence of SO<sub>2</sub> on the interaction of NO<sub>2</sub> with the unpaired electrons of soot. These data are consistent with the displacement of some adsorbed SO<sub>2</sub> by NO<sub>2</sub>, however, as indicated by the microgravimetric data of Figure 4. This does not account for any presence of O<sub>2</sub> in zero air and its occupation of free radical sites, which would be reflected microgravimetrically in changes in capacity for SO<sub>2</sub> under some conditions.

Separate experiments have shown that soot treated with 140 torr NO<sub>2</sub>, resulting in a reduction of CNI from  $1.62 \times 10^7$  to  $0.61 \times 10^7$ , undergoes an increase of 10% in unpaired spins upon exposure to air. Evacuation at  $10^{-6}$  torr further increases the CNI to  $1.05 \times 10^7$  while the addition of air returns it to  $0.67 \times 10^7$ , the cycle continuing to change the spin density of carbon in this manner. It appears that O<sub>2</sub> does compete effectively with the small physisorbed fraction (~10%) of adsorbed NO<sub>2</sub> for

unpaired electron sites.

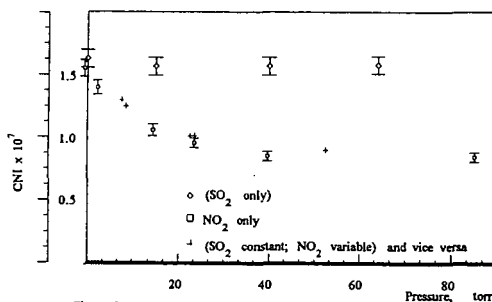


Figure 5. CNI against gas pressure

#### NO Adsorption

The FT-IR evidence presented for the lack of NO reactivity with soot at ambient temperatures (3) is supported by EPR studies of NO and NO + O<sub>2</sub> adsorption. Figure 6 shows the effects of O<sub>2</sub> and

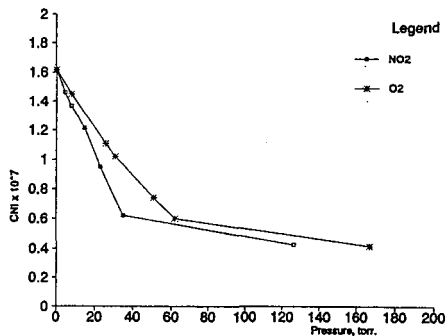


Figure 6. Effects of oxidants on the normalized integral of soot.

NO adsorption on the CNI of soot beyond a linear range below 50 torr to pressures of nearly 170 torr. The similar but slightly lesser effect of NO on spin density, as compared with that of O<sub>2</sub>, forms the basis for the experiments summarized in Figure 7. Exposure of the soot to air following adsorption of NO at 8 and 62 torr shows the effect on CNI expected below and at / or above surface saturation by NO, respectively. The surprising effect is the more complete removal of paramagnetic species NO + O<sub>2</sub> to yield a higher CNI than the initial. This consistent result shows NO-assisted removal of that O<sub>2</sub> still remaining on the soot surface following the initial evacuation and mild thermal treatment. It is to be contrasted with the similar experiment with NO<sub>2</sub> described above. NO apparently is reversibly adsorbed and, probably through formation of a complex (or reaction) with pore O<sub>2</sub>, even raises the spin density of the soot through its evacuation.

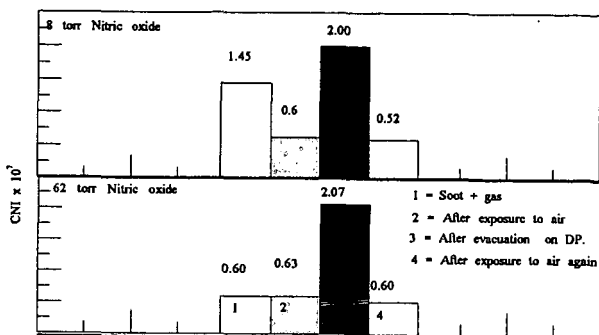


Figure 7 . Plot of CNI for Soot/gas-Air exposure-Evacuation-Exposure to air sequence .

#### ACKNOWLEDGEMENTS

The authors gratefully acknowledge the support of the National Science Foundation for this research through grant ATM-9200923. Gratitude also is expressed to S. S. and G. R. Eaton of the Department of Chemistry for assistance with, and for the use of, the EPR instrumentation.

#### REFERENCES

1. Akhter, M. S.; Chughtai, A. R.; Smith, D. M., *J. Phys. Chem.*, 1984, 88, 5334.
2. Chughtai, A. R.; Gordon, S. A.; Smith, D. M., *Carbon* 1994, 32, 405.
3. Smith D. M.; Welch, W. F.; Graham, S. M.; Chughtai, A. R.; Wicke, B. G.; Grady, K. A., *Appl. Spectrosc.* 1988, 42, 674.
4. Chughtai, A. R.; Welch, W. F.; Akhter, M. S.; Smith, D. M., *Appl. Spectrosc.* 1990, 44, 294.
5. Chughtai, A. R.; Welch, W. F.; Smith, D. M., *Carbon* 1990, 28, 411.
6. Smith D. M.; Keifer, J. R.; Novicky, M.; Chughtai, A. R., *Appl. Spectrosc.* 1989, 43, 103.
7. Chughtai, A. R.; Brooks, M. E.; Smith, D. M., *J. Geophys. Res.*, 1995, in press.
8. Smith D. M.; Atteya, M. M. O.; Konowalchuk, B. K.; Rosenberger, M. L.; and Chughtai, A. R., *Symposia Preprints, Div. Fuel Chemistry, Am. Chem. Soc., New Orleans*, 1996.
9. Billinge, B. H. M., in *Second Conference on Industrial Carbon and Graphite*, Society of Chemical Industry, London, 1966; p. 399.
10. Hayward, D. O.; Trapnell, B. M. W., *Chemisorption*, 2nd ed., Butterworths, London, 1964, p. 167.
11. Davini, P., *Carbon*, 1994, 32, 349.